International Journal of Mechanical And Production Engineering, ISSN: 2320-2092, Volume- 5, Issue-8, Aug.-2017
http://iraj.in

THERMO MECHANICAL TREATMENT OF DUPLEX SAF 2507 STEEL

[1]PETR MARTINEK, [2]MICHAL DUCHEK, [3]IVANA POLAKOVA

COMTES FHT, A.S.
E-mail: petr.martinek@comtesfht.cz, michal.duchek@comtesfht.cz, ivana.polakova@comtesfht.cz

Abstract- This contribution deals with thermo mechanical treatment of SAF 2507 duplex steel. The purpose of the treatment was to achieve the desired shape and hardness of the work piece. It was intended to use a hardness contribution from precipitates of inter metallic phases. Since inter metallic precipitation is very sensitive to the forging temperature and post-forging cooling rate, the entire forging process and post-forging treatment route was first simulated using numerical modelling. Above all, the rate of cooling after forging was monitored at several pre-defined points because it has a major effect on the resulting microstructure and mechanical properties in duplex steel. The presence of inter metallic phases was detected using optical and scanning electron microscopy. Their types were identified by means of EBSD analysis. As inter metallic precipitation causes severe embrittlement, notch impact toughness was measured upon individual experiments.

Index Terms- Thermo mechanical treatment, numerical simulation, duplex steel, EBSD analysis

I. INTRODUCTION

Duplex stainless steels are frequently used in industry for their excellent combination of mechanical properties and corrosion resistance [1]. Their resistance to uniform corrosion is similar to austenitic steels but their strength is much higher [2].
Processing at high temperatures, such as forging, extrusion or rolling is critical for duplex steels due to formation of precipitates of deleterious phases - namely sigma phase [3]. Sigma phase is one of very common intermediate phases, being hard brittle, non-magnetic and stable. Precipitation of sigma phase in steel substantially reduces toughness, elongation and reduction of area in tensile test, which becomes more severe with the growing volume fraction [4].

On the other hand, precipitation of sigma phase is induced on purpose in some cases, because it also increases yield strength, ultimate tensile strength and hardness. With its high chromium content, sigma phase can provide passivation, and therefore does not substantially compromise the properties of passivated corrosion-resistant steels. Formation of sigma phase depends on chemical composition and treatment route and is in direct proportion to the non-uniformity of chromium distribution. In austenitic-ferritic steels, the amount of sigma phase is always larger than in pure austenitic steels. The tendency toward precipitation of sigma phase is directly proportional to the amount of ferrite [5, 6]. Sigma phase precipitates first at triple junctions, then at grain boundaries and, upon longer time at higher temperatures, on non-coherent grain boundaries and inclusions within grains. [7]
The goal of this experiment was to increase the surface hardness of a forged workpiece to 300 HV by thermomechanical treatment involving incomplete precipitation of sigma phase. It was motivated by the fact that the workpiece is used for making parts that operate in a corrosive and abrasive environment, which is why its surface hardness must be at least 300 HV.

II. NUMERICAL MODELLING

In order to determine and compare cooling rates achieved by individual cooling methods, the entire forging and post-forging heat treatment route was simulated using numerical methods. The DEFORM 3D Multiple Operations software was used which, among other data, offers information on the material flow, strain rate and strain magnitudes during forming, and on temperatures during handling and forming. [8] Basic material data were determined by means of JMatPro software.
The focus on the cooling rate from the finishing temperature was motivated by the fact that it has a major impact on intermetallic precipitation [9]. Two cooling methods were simulated: cooling in water bath and cooling by water spray. The starting conditions for the simulations of post-forging cooling comprised the surface temperature of the forged piece of 1050°C and its mid-thickness temperature of 1200°C (Fig. 1). In the second production route simulated, the workpiece was reheated in a furnace to 1250 °C upon forging. The handling time for the transfer from the furnace to the cooling environment was 1 min.

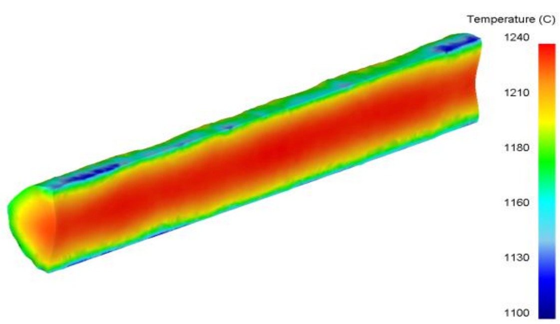

Fig. 1. Workpiece temperature field just after forging

The reference points for numerical modelling were located on the workpiece surface (P1), 10 mm below the surface (P2) and in the workpiece centre (P3). Calculated cooling rates are plotted in the graphs (Fig. 2 and Fig. 3).

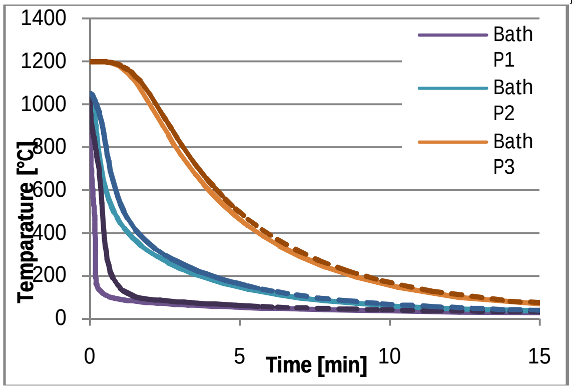

Fig. 2. Simulated route 1 – post-forging cooling

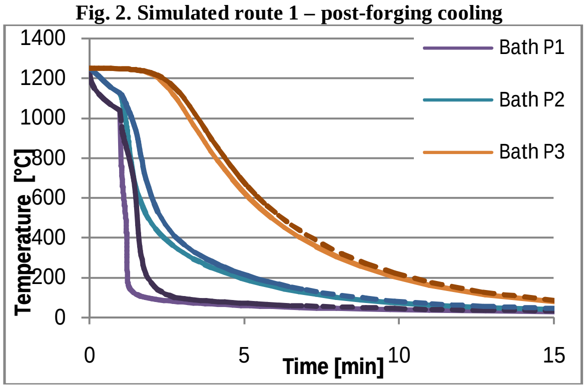

Fig. 3. Simulated route 2 – cooling of a workpiece with uniform temperature of 1250°C

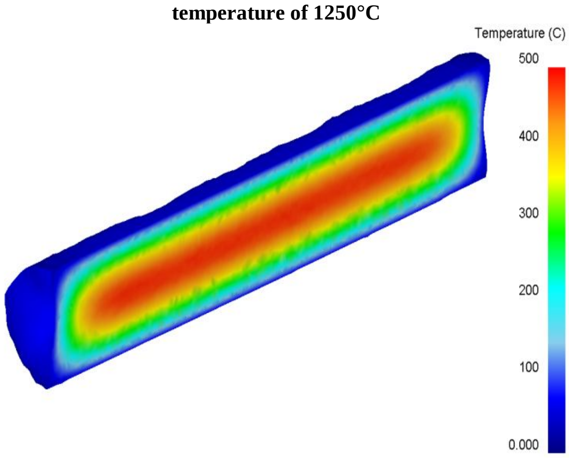

Fig. 4. Workpiece temperature distribution 6 minutes into the water spray-cooling process, i.e. 7 minutes after the workpiece was removed from a furnace at 1250°C

The findings from numerical modelling became a basis for designing real-life forging experiments.

III. EXPERIMENTAL PROGRAMME

The feedstock for forging was a rod of 200 x 500 mm cross section from SAF 2507 material (Table 1). It was forged into a round bar of 140 mm diameter. The desired surface hardness of the forged workpiece 300 HV. The forging experiments were carried out at the company COMTES FHT a.s. Three experiments were designed on the basis of the numerical simulations.
In the first one, the workpiece was cooled in water bath immediately after the last forging operation. Its surface temperature was around 1050°C and its calculated mid-thickness temperature was 1200°C.
In the second experiment, the workpiece was reheated in a furnace to 1250°C after forging. It was then cooled in a special water-spray conveyor of 3-metre length where the spray intensity on both sides can be controlled. The transfer to the conveyor took 1 minute, as planned.
The purpose of the third experiment was to map the extent of precipitation of deleterious phases during workpiece cooling in air. From this workpiece, experimental specimens were taken and the rest of the workpiece was solution-annealed at 1080°C and then cooled in water bath in order to restore toughness in the duplex steel [10].

Table. 1. Chemical compositions of experimental steels

Element	C	Si	Mn	P	S
wt. %	0.021	0.255	0.759	0.023	0.015
Element	Cr	Mo	Ni	Cu	Al
wt. %	24.26	3.55	6.71	0.102	0.017

IV. METALLOGRAPHIC ANALYSIS

Metallographic specimens were prepared from the workpieces after each experiment. The specimens were prepared using a standard metallographic procedure involving grinding and subsequent polishing. Microstructures were revealed by etching with Beraha II reagent with an addition of $K_2S_2O_5$. This reagent colours ferrite brown or blue, whereas austenite remains bright. The microstructures were documented using NIKON EPIPHOT 200 optical microscope. Detail micrographs were taken using the scanning electron microscope JEOL 6380 using secondary electron imaging.
A. Experiment 1 – Water bath cooling upon forging
In this experiment, the workpiece was cooled in water bath immediately after the last forging operation. Microstructures were examined in the centre of the workpiece and near its surface. There was no appreciable difference between these locations where the microstructures consisted of δ-ferrite and austenite. The distributions of both phases were uniform and their area fractions were equal (Fig. 5). No intermetallic phases were found using optical microscopy or scanning electron microscopy (Fig. 6).

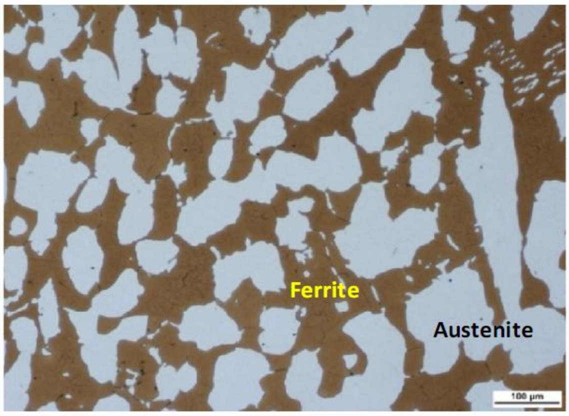

Ferrite

Fig. 5. Forged workpiece after cooling in water bath, centre, 100×

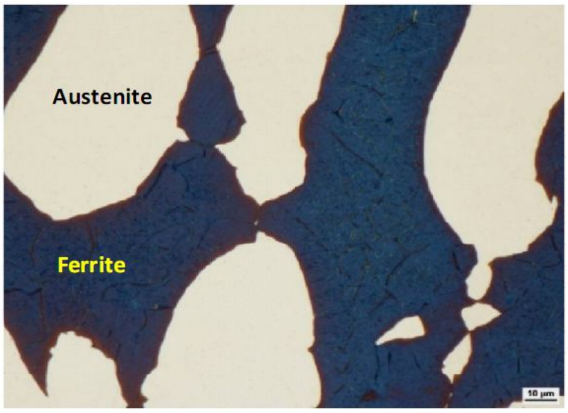

Fig. 6. Forged workpiece after cooling in water bath, near-surface region, 500×

B. Experiment 2 – Water spray cooling from 1250°C

After forging, the workpiece was placed in a furnace and reheated to 1250°C. Afterwards, it was transferred within one minute to a water spray conveyor where it was cooled with water.

Its microstructure comprised δ-ferrite and austenite as well, but it also contained intermetallic particles (Fig. 7 and Fig. 8). These were found in both the sub-surface location and the centre of the workpiece.

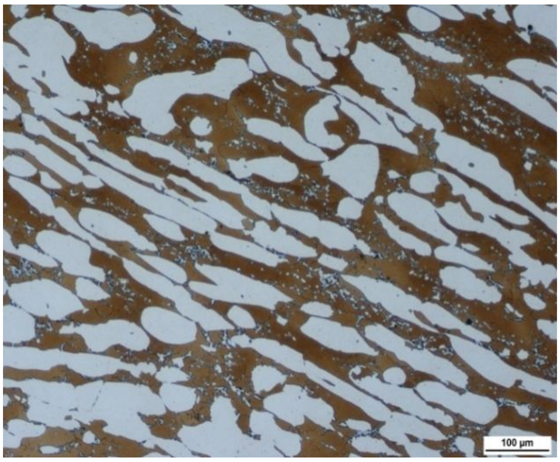

Fig. 7. Forged workpiece after cooling with water spray, near-surface region, 100×

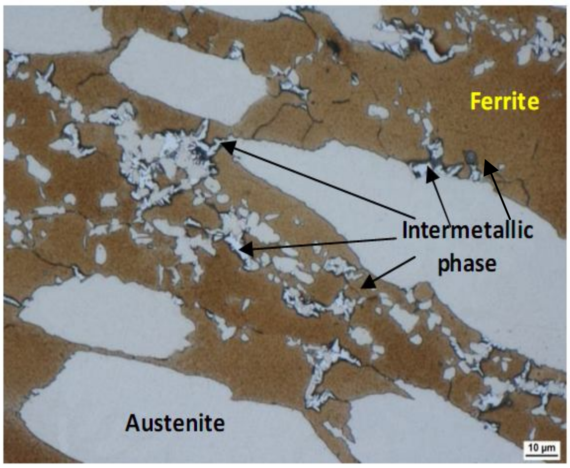

Fig. 8. Forged workpiece after cooling with water spray, near-surface region, 500×

In the specimen taken from a near-surface region, intermetallic particles are only present at the austenite-δ-ferrite interface (Fig. 9). By contrast, in the specimen from the workpiece centre, intermetallic particles are found both at the inter-phase interface and within ferrite grain.

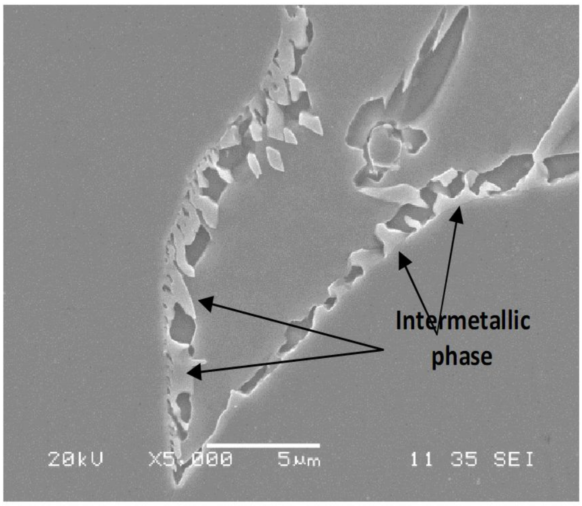

Fig. 9. Forged workpiece after cooling with water spray, near-surface region, 5000×

C. Experiment 3 – Air cooling upon forging

This forged workpiece cooled in air after finishing. The microstructure in the centre consists, again, of δ-ferrite and austenite, with intermetallic particles found mostly at the inter-phase interface (Fig. 10). In the centre of this workpiece, the microstructure is similar to that of the workpiece in experiment 2. Their hardness levels are similar as well: around 300 HV10.

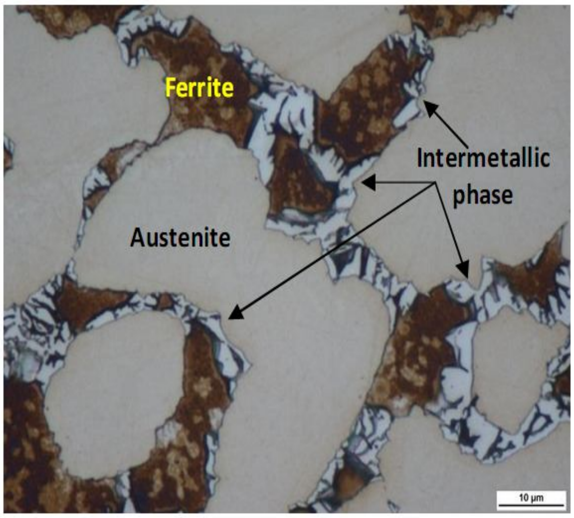

Fig. 10. Air-cooled after forging, centre, 1000×

Near the workpiece surface, massive precipitation of intermetallic particles occurred (Fig. 11). As a result, δ-ferrite was completely replaced with a mixture of austenite and intermetallic phases, the latter dominated by apparently by sigma phase. Larger isolated δ-ferrite islands are scarce in this microstructure (Fig. 12 and Fig. 13).

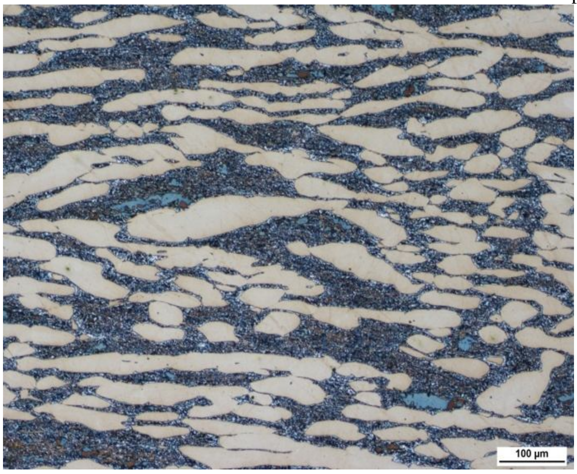

Fig. 11. Air-cooled after forging, near-surface region, 100×

Fig. 12. Air-cooled after forging, near-surface region, 500×

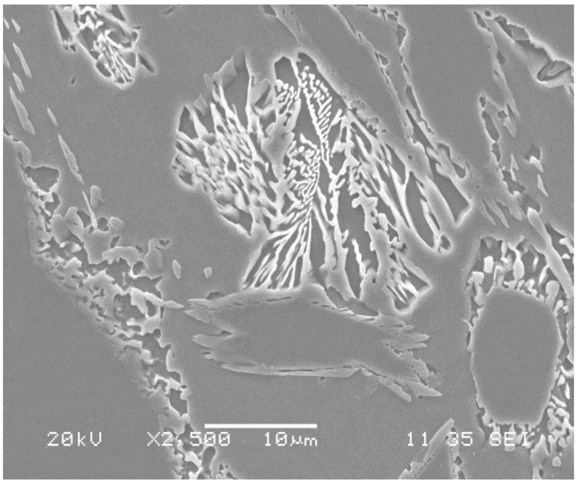

Fig. 13. Air-cooled after forging, near-surface region, 2500×

D. Experiment 3-1 – Workpiece after solution annealing

During experiment 3, massive precipitation of intermetallic phases occurred. As a consequence, the steel lost toughness, became brittle and its hardness rose above the required level. In response to this, additional solution annealing was carried out. The annealing temperature and time were 1080°C and 1 hour, respectively, and the workpiece was then cooled in water bath.

Upon annealing, the microstructure consisted only of δ-ferrite and austenite; no intermetallic particles were found either under optical microscope or in a scanning electron microscope (Fig. 14).

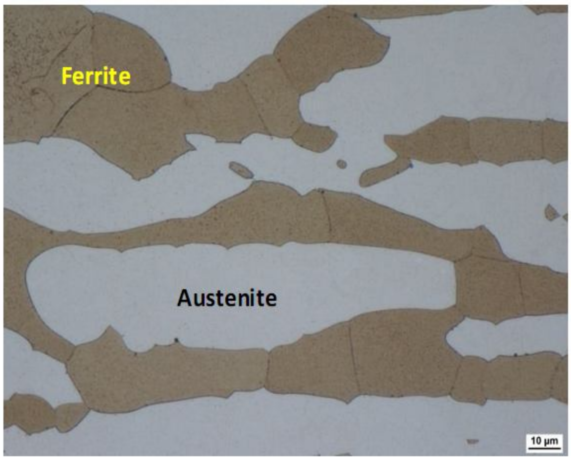

Fig. 14. Microstructure upon solution annealing, 500×

E. EBSD analysis of intermetallic phases

The intermetallic phases were identified using EBSD analysis. The analysis was carried out in a JEOL JSM-7400 microscope equipped with an EBSD camera from OXFORD Instruments. In the specimen from experiment 1, only ferrite and austenite were identified. No intermetallic particles have been found (Fig. 15). The same findings were made with the specimen from experiment 3-1. In the specimen from experiment 2, sigma phase and chi phase particles were identified, in addition to austenite and δ-ferrite (Fig. 16). Both phases are hard, brittle and can lead to embrittlement. Although the number of intermetallic particles evaluated was not sufficient to be representative, it appears that the fractions of the sigma and chi phases are roughly equal. In the specimen from experiment 3, sigma and chi phase particles were found as well. Nevertheless, the amount of sigma phase was much larger than that of chi phase, whose particles were rare. In this specimen, $M_{23}C_6$ carbides were identified.

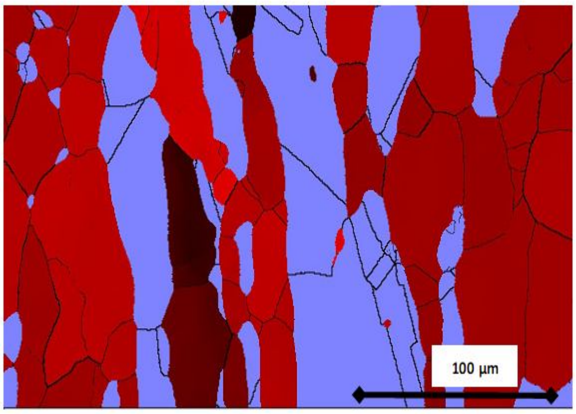

Fig. 15. Experiment 1, EBSD map of ferrite orientation (red colour); austenite shown in blue

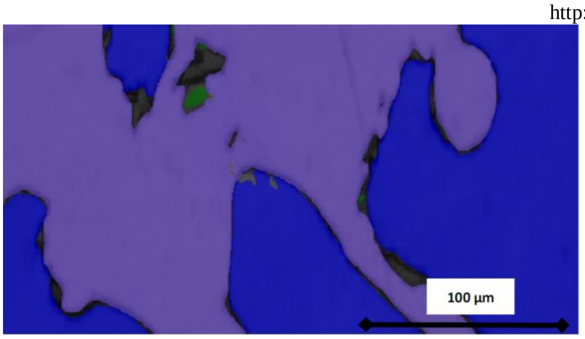

Fig. 16. Experiment 2, EBSD map of ferrite orientation (purple colour); austenite shown in blue, chi phase in green

V. IMPACT TEST

Charpy impact toughness test was carried out in accordance with ČSN ISO 148-1. The test temperature was 20°C. In each case, three specimens were tested. Table 2 gives calculated mean values.

Table. 2. Impact toughness test values

Specimen	KV_2	KCV
	[J]	[J/cm^2]
Experiment 1 – Water bath cooling upon forging	223.7	279.9
Experiment 2 – Water spray cooling from 1250°C	55.8	70.1
Experiment 3 – Air cooling upon forging	1.6	2.0
Experiment 3-1 – experiment 3 + solution annealing	292.4	366.2

VI. HARDNESS TEST

Hardness was measured by means of a Struers DuraScan laboratory hardness tester. The desired surface hardness of the workpiece was 300 HV. Hardness readings were taken on all experimental specimens. Table 3 shows calculated mean values from five measurements.

Table. 3. Hardness values [HV10]

Specimen	Location	Hardness
Experiment 1 – Water bath cooling upon forging	Centre	254
	Surface	264
Experiment 2 – Water spray cooling from 1250°C	Centre	287
	Surface	308
Experiment 3 – Air cooling upon forging	Centre	424
	Surface	298
Experiment 3-1 – experiment 3 + solution annealing	Centre	267
	Surface	273

CONCLUSION

The goal of this experiment was to increase the surface hardness of a forged workpiece to 300 HV by thermomechanical treatment involving incomplete precipitation of sigma phase.

In specimens from experiment 1, where the workpiece was cooled in water bath immediately after the last forging operation, no intermetallic particles were found. Its hardness was near 260 HV10 and its notch toughness represented by impact energy was high: 223.7 J.

Unlike in the previous specimens, in those from the second experiment, where the workpiece was reheated in a furnace to 1250°C after forging and then cooled in a special water-spray conveyor, intermetallic precipitates were found. EBSD analysis identified sigma phase and chi phase. The surface hardness of this workpiece reached 308 HV10, and the requirement for the surface hardness of at least 300 HV was thus met. At the same time, however, the intermetallic precipitation led to a drop in notch toughness, as the impact energy was 55.8 J.

In specimens from the third experiment, where the workpiece cooled in air after forging, extensive intermetallic precipitation was detected, predominantly near the surface. Mechanical working and the introduced deformation energy greatly accelerated the formation of intermetallic phases. As a result, the near-surface regions of the forged bar contained much larger amounts of intermetallic phases than the centre, although the temperature field would lead one to believe that greater amounts of intermetallic phases would precipitate in the centre of the part. EBSD analysis revealed them as mainly sigma phase particles, although some chi phase and chromium carbide particles were found as well. Hardness near the surface of the workpiece rose to 424 HV10 but the material lost toughness completely, as the impact energy was no more than 1.6 J.

Solution annealing of the material from experiment 3 dissolved all intermetallic particles, hardness decreased to approx. 270 HV10 and toughness returned to a high level represented by the impact energy of 292.4 J.

The measurement suggests that hardness and impact toughness in duplex steel is governed by the amount of intermetallic precipitates – which can be controlled by post-forging thermal conditions. The desired surface hardness of 300 HV was obtained in the second experiment which involved water spray cooling. In addition, the impact toughness was acceptable.

ACKNOWLEDGEMENTS

This paper was created by project Development of West-Bohemian Centre of Materials and Metallurgy No.: LO1412, financed by the MEYS of the Czech Republic.

REFERENCES

[1] J. M. Cabrera, et al., “Hot deformation of duplex stainless steels“, Journal of Materials processing Technology, Volumes 143-144, 20 December 2003, Pages 321-325

[2] J. O. Nilsson, “Super duplex stainless steels“. Material Science and Technology, 1992, vol. 8, pp. 685–700.

[3] M. Balcar, L. Sochor, J. Novak, L. Martinek, P. Fila, J. Svatoň, V. Turecky, P. Martinek, P. Podany, J. Bažan. “Production and Heat Treatment of Duplex Stainless Steel Forgings, METAL 2012 Conference Proceedings, ISBN 978-80-87294-31-4

[4] H. Sieurin, R. Sandström, "Sigma phase precipitation in duplex stainless steel 2205". Material Science and Engineering, 2007, vol. 444, no. 1, pp. 271-276.
[5] Lagneborg R. Jonson R., "Stainles steel in the 90's Materials & design", Volume 10, Issue 3, May-June 1989, Pages 144-152
[6] C.S. Huang, C. C. Shih, "Effects of nitrogen and high temperature aging on σ phase precipitation of duplex stainless steel". Material Science and Engineering, 2005, vol. 402, no. 8, pp. 66–75.
[7] P. Podany, J. Dlouhy, M. Köver, "Effect of ageing on phase evolution and precipitation behaviour of duplex steel" IOP Conference Series: Materials Science and Engineering, Volume 103, 4th Global Conference on Materials Science and Engineering (CMSE 2015. Aug 04, 2015, Macau, UK. Bristol, 2015. p. 7. ISSN 1757-899X
[8] I. Polakova, T. Kubina, "Flow Stress Determination Methods for Numerical Modelling". In: METAL 2013. May 15, 2013, Brno, CZ. Ostrava. p. 6 / 273-278. ISBN 978-80-87294-41-3
[9] T. Maki, T. Furuhara, K. Tsuzaki, "Microstructure development by thermomechanical processing in duplex stainless steel". ISIJ International, 2001, vol. 41, pp. 571–579.
[10] P. Martinek, J. Miskova, J. Dlouhy, P. Podany, M. Balcar, "Impact of Solution Annealing on Properties of Duplex Steel", 25th Anniversary International Conference on Metallurgy and Materials, METAL 2016 Conference Proceedings, ISBN 978-80-87294-67-3

★★★